

Isospin mixing in the ^{60}Zn nucleus

G. GOSTA⁽¹⁾⁽²⁾

⁽¹⁾ *INFN, Sezione di Milano - Milano, Italy*

⁽²⁾ *Dipartimento di Fisica, Università degli Studi di Milano - Milano, Italy*

received 25 January 2021

Summary. — An experimental study of the isospin mixing for the ^{60}Zn nucleus was made by measuring the γ -decay from the Giant Dipole Resonance. Two compound nuclei, ^{60}Zn and ^{62}Zn , were populated at two different excitation energies, $E^* = 47$ MeV and $E^* = 58$ MeV, using the fusion evaporation reactions $^{32}\text{S} + ^{28}\text{Si}$, at the bombarding energy of 86 MeV and 110 MeV, and $^{32}\text{S} + ^{30}\text{Si}$, at 75 MeV and 98 MeV. The ^{62}Zn nucleus was used as a reference. In the experiment, performed at the LNL-INFN laboratory, the γ -rays were measured with the GALILEO detection system in which large-volume $\text{LaBr}_3(\text{Ce})$ detectors were added to the HPGe detectors. The Coulomb spreading width was obtained from the comparison of the two reactions. The isospin-mixing coefficient at zero temperature, of the order of 2.5%, was deduced and the measured value agrees with that from mass and beta-decay measurements and with theory. The isospin-symmetry-breaking correction δ_c used for the Fermi super-allowed transitions was also extracted from the value of the isospin impurity.

1. – Introduction

One basic symmetry of the strong nuclear force is the isospin symmetry, introduced to describe the interaction between nucleons and which is known to be broken by the Coulomb interaction. This symmetry manifests itself also in the structure of nuclei and in nuclear reactions. This breaking affects the properties of the β -decay [1, 2] and of the Isobaric Analogue State (IAS) [3]. Particular effort is being made to deduce the value of isospin mixing for nuclei in different mass regions [4, 5]. Tools are the selection rules for the electric dipole ($E1$) transition in self-conjugate nuclei [6] and the β Fermi transition between states with different isospin values [7].

The isospin symmetry was introduced by Heisenberg in 1932, to cope with the experimental finding of the charge symmetry and the charge independence of the nucleons interaction, namely, the n - n , p - p and n - p interactions are the same. In the isospin formalism, neutrons and protons are viewed as two quantum states of the same particle, the nucleon, with isospin projection $|I_z| = 1/2$ and $|I_z| = -1/2$ for proton and neutron,

respectively. Consequently, a nucleus has a well-defined value of $|I_z| = (N - Z)/2$, while I , according to quantum mechanics rules, can assume values $(N - Z)/2 < I < (N + Z)/2$. In general, for $N = Z$ nuclei, the nuclear ground state corresponds to the lower value of the isospin $I = |I_z|$. This symmetry does not hold for the Coulomb interaction between protons in the nucleus and this leads to a breaking of the symmetry which induces a mixing between states with different values of isospin. This phenomenon is called ‘‘isospin mixing’’. The consequence is that it is not possible to assign a unique value of isospin to a nuclear state A , that must be described as a superposition of two or more states with different isospin values:

$$(1) \quad |A\rangle = \alpha|I\rangle + \beta|I + 1\rangle.$$

Because the nuclear force overwhelms the Coulomb interaction, a perturbation approach can be used to describe the isospin mixing. In first-order perturbation theory, the probability of having an admixture of $I = I_0 + 1$ states into $I = I_0$ ones, indicated by α^2 , is defined as

$$(2) \quad \alpha^2 = \sum_{I_0+1 \text{ states}} \frac{|\langle I = I_0 + 1 | H_c | I_0 \rangle|^2}{(E_{I_0+1} - E_{I_0})^2},$$

where H_c is the Coulomb Hamiltonian. From eq. (2) we can deduce that a large matrix element can occur only between states with very similar level energy and similar wave functions. To describe the isospin mixing in a compound nucleus we need to refer to the Morinaga and Wilkinson hypothesis [8] for which the coefficient α^2 is defined as the ratio between the Coulomb spreading width and the compound nucleus decay width, that in terms of time, is the compound nucleus lifetime over the timing necessary for the isospin mixing of states:

$$(3) \quad \alpha^2 \approx \frac{\Gamma_c^\downarrow}{\Gamma_{CN}} = \frac{\tau_{CN}}{\tau_c^\downarrow}.$$

Morinaga and Wilkinson suggested that at high nuclear temperatures the isospin symmetry becomes a better symmetry. At high excitation energies, indeed, the compound nuclear decay width becomes large, overwhelming the Coulomb interaction matrix element; thus, the nucleus decays before the isospin degrees of freedom have time to equilibrate. This implies the restoration of the symmetry. Thus, a dynamical behaviour between the Coulomb interaction time-scale and the compound nucleus lifetime is at play.

2. – The experiment

The isospin is not an observable that can be measured directly, but we can measure the effect of the symmetry on the nuclear system. The way we used to determine the isospin-mixing coefficient is to study a γ -decay that would be forbidden by the selection rules of the isospin symmetry, if the isospin were a good quantum number. In the study here presented the compound nucleus ^{60}Zn was formed by a fusion-evaporation reaction,

namely $^{32}\text{S} + ^{28}\text{Si} \rightarrow ^{60}\text{Zn}^*$, with a bunched beam of ^{32}S (intensity ≈ 2 pA) and a self-supporting target of ^{28}Si ($400 \mu\text{g}/\text{cm}^2$). The experiment was performed at the Laboratori Nazionali di Legnaro (LNL).

Both the projectile and the target have, respectively, the same number of protons and neutrons ($N = Z$), therefore, the nucleus of interest ^{60}Zn is created in an $I = 0$ state. For the selection rules, the electric dipole transitions in the long-wavelength limit are forbidden between states of same isospin, thus, the nucleus can not decay to a state of $I = 0$ but it can decay to a state of $I = 1$. The density of $I = 0$ levels is always higher than the density of $I = 1$ levels, therefore, if the compound nuclear isospin is pure, the production of high-energy γ -rays in $I = 0$ compound nuclear entrance channels should be reduced compared to that of $I \neq 0$ entrance channels [9]. Thus, from the experimental point of view, the decay should be barely visible. If we assume the breaking of the symmetry and that the nucleus is formed in a state which is composed by the mixing of two states (at the first order), $I = 0$ and $I = 1$, the $E1$ decay becomes possible. The $I = 1$ part of the initial state can decay to the $I = 0$ state. The strength of the $E1$ decay is almost totally concentrated in the Giant Dipole Resonance (GDR) and the measurement of the yield of this decay provides information on the isospin-mixing coefficient.

The GDR in nuclei at finite T and angular momentum was investigated in many experimental and theoretical works and, thus, a solid base exists for the use of this approach [10-13]. At a finite temperature, one expects a partial restoration of the isospin symmetry because the degree of mixing in a CN is limited by its finite lifetime, as predicted by Wilkinson [8]. Because the isospin-mixing probability is a quantity of the order of a few percent, we need a second reaction, which is not affected by the mixing effect, to use as a reference. This reaction creates a very similar compound nucleus with very similar excitation energy and angular momentum but in a non-zero state of the isospin. The $^{32}\text{S} + ^{30}\text{Si} \rightarrow ^{62}\text{Zn}^*$ reaction at bombarding energies of 75 MeV and 98 MeV was measured and used to fix the GDR parameters. Both nuclei were formed at 2 different excitation energies, $E^* = 47$ MeV and $E^* = 58$ MeV (corresponding to nuclear temperatures $T = 2$ MeV and $T = 2.4$ MeV), to study the isospin-mixing dependence on temperature. The same experimental technique was used in previous works on ^{80}Zr [14, 15] and on ^{32}S [16].

For this measurement, an experiment in 2016 and a second data taking in 2018 were performed, because in the first case a contamination of oxygen in the target was found. The second measurement was made for further check, even if the effect of the contamination in the GDR region was not strong. A complex experimental set-up was assembled in order to allow the measurement of both γ -rays and particles emitted during the decay of the compound nucleus. The main part of the set-up consisted in the GALILEO array [17] including 25 HPGe detectors, coupled to an array of 10 $\text{LaBr}_3(\text{Ce})$ scintillator detectors [18]. In addition, an array of 40 silicon detectors in $E - \Delta E$ telescopes configuration, EUCLIDES [19], and an array of 15 BC501A scintillator detectors, named Neutron Wall [20], were installed in the set-up. The HPGe detectors were used to measure the low-energy γ -rays (up to 4 MeV) useful for the identification of the residual nuclei emitted during the decay of the compound nucleus, while the $\text{LaBr}_3(\text{Ce})$ detectors, with the capability to measure high-energy γ -rays, were used to measure the GDR. The two ancillary arrays, EUCLIDES and Neutron Wall, were used to detect charged particles and neutrons, respectively. In the lower panel of fig. 1, the HPGe spectrum for the $^{32}\text{S} + ^{28}\text{Si} \rightarrow ^{60}\text{Zn}^*$ reaction at $T = 2.4$ MeV is presented. We identified the main residual nuclei produced during the compound nucleus decay: ^{57}Co , ^{56}Co , ^{51}Mn , ^{53}Mn and ^{54}Fe , whose transitions are indicated with different symbols in the figure.

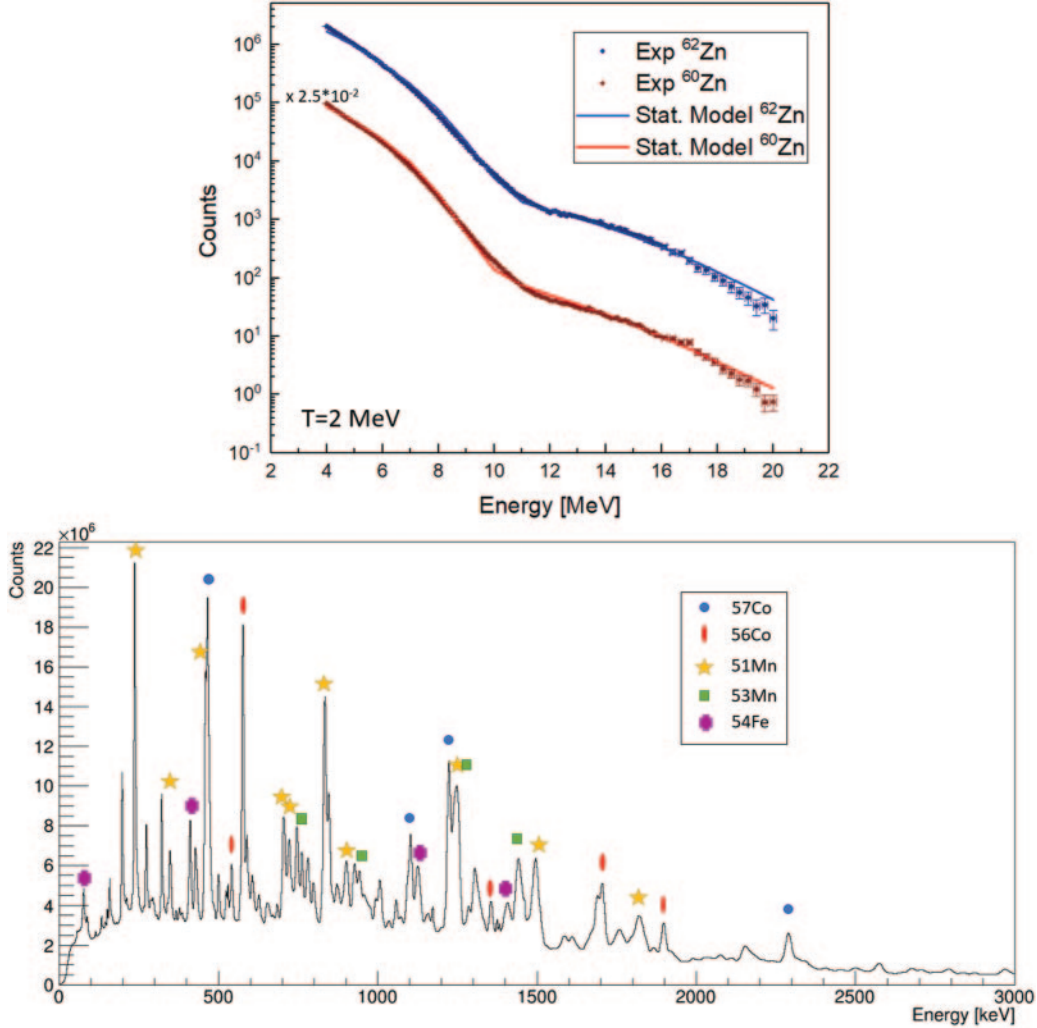


Fig. 1. – Upper part: Experimental spectra for ^{62}Zn (blue points) and ^{60}Zn (red points), together with the best fits with the statistical model for ^{62}Zn (blue line) and ^{60}Zn (red line). Lower part: HPGe spectrum for the $^{32}\text{S} + ^{28}\text{Si} \rightarrow ^{60}\text{Zn}^*$ reaction at $T = 2.4$ MeV. Transitions belonging to the main residual nuclei produced during the compound nucleus decay (*i.e.*, ^{57}Co , ^{56}Co , ^{51}Mn , ^{53}Mn , ^{54}Fe) are indicated with different symbols.

3. – Results

The data analysis used the statistical model and was mainly based on three steps: i) the fit of GDR parameters (strength, width and centroid) using the ^{62}Zn data; ii) the application of the GDR parameters to the ^{60}Zn spectrum and the fit of the Coulomb spreading width as the only free parameter; iii) from the Coulomb spreading width, the extraction of the mixing probability. The original version of the statistical model code, named CASCADE [21], has been modified first from Harakeh [9] and then by the Washington University group [22], in order to implement the isospin symmetry.

TABLE I. – GDR parameters obtained for ^{62}Zn at $T = 2 \text{ MeV}$ and $T = 2.4 \text{ MeV}$.

| Temperature | E_{GDR} (MeV) | Γ_{GDR} (MeV) | S_{GDR} (%) |
|-------------|------------------------|-----------------------------|----------------------|
| 2 MeV | 18.4 ± 0.1 | 11.6 ± 0.2 | 90 |
| 2.4 MeV | 18.1 ± 0.1 | 12.6 ± 0.2 | 90 |

3'1. Fit of GDR parameters. – The statistical model provides the γ -ray spectrum produced during the decay of a CN, which was compared with the experimental data of ^{62}Zn . The statistical model spectra were folded with the detector response function and normalized to the experimental data at around 5–6 MeV. Because of the exponential nature of the spectra, the fit minimization (between 12 and 17 MeV) was applied to a Figure Of Merit (FOM) defined dividing the standard χ^2 over the number of counts [11]. To consider, in the fitting process, the statistical error of the experimental spectrum, 10^4 spectra were created adding to the number of the experimental counts a fluctuation randomly extracted from a Gaussian distribution centred at zero and with a standard deviation equal to the statistical error on the number of counts per bin ($\sigma = \sqrt{Y_i}$). Each of the 10^4 spectra was compared with n CASCADE simulations, varying in GDR parameters, centroid and width, while the strength was fixed at 90%, as in the literature. The GDR parameters obtained following this procedure are listed in table I. In the upper part of fig. 1, the experimental points of ^{62}Zn (blue points), at $T = 2 \text{ MeV}$, are compared with the statistical model simulation that represents the best fit (blue line).

3'2. Fit of Coulomb spreading width. – The isospin mixing is included in the statistical model code according to the parametrization of Harney, Richter and Weidenmüller [23], in which the mixing between the states $I_{<} = I_0$ and $I_{>} = I_0 + 1$ is considered, and where I_0 is the initial CN state. At high excitation energy, the compound nucleus exhibits a decay width $\Gamma_{\gtrsim}^{\uparrow}$ and the mixing probability, α_{\gtrsim}^2 , of states \gtrsim in states \lesssim can be defined as

$$(4) \quad \alpha_{\gtrsim}^2 = \frac{\Gamma_{\gtrsim}^{\downarrow}/\Gamma_{\gtrsim}^{\uparrow}}{1 + \Gamma_{\gtrsim}^{\downarrow}/\Gamma_{\gtrsim}^{\uparrow} + \Gamma_{\lesssim}^{\downarrow}/\Gamma_{\lesssim}^{\uparrow}},$$

where $\Gamma_{\gtrsim}^{\downarrow}$ is the Coulomb spreading width of the states \gtrsim . $\Gamma_{\gtrsim}^{\downarrow}$ are rather constant with excitation energy while $\Gamma_{\gtrsim}^{\uparrow}$ increase rapidly, thus a partial restoration of isospin symmetry at high excitation energy is expected. For the statistical model analysis of the spectrum associated to ^{60}Zn , the Coulomb spreading width is considered as the only free parameter since the GDR values were fixed from the ^{62}Zn analysis. Following the same procedure used for ^{62}Zn , we produced 10^4 spectra adding the fluctuation randomly extracted from a Gaussian distribution and we compared all of them with CASCADE simulations, varying the Coulomb spreading width from 0 to 50 keV. The Coulomb spreading width that best fits the experimental points was obtained from the minimization of the χ^2 of the ratio $^{60}\text{Zn}/^{62}\text{Zn}$. This approach reduces the possible systematic

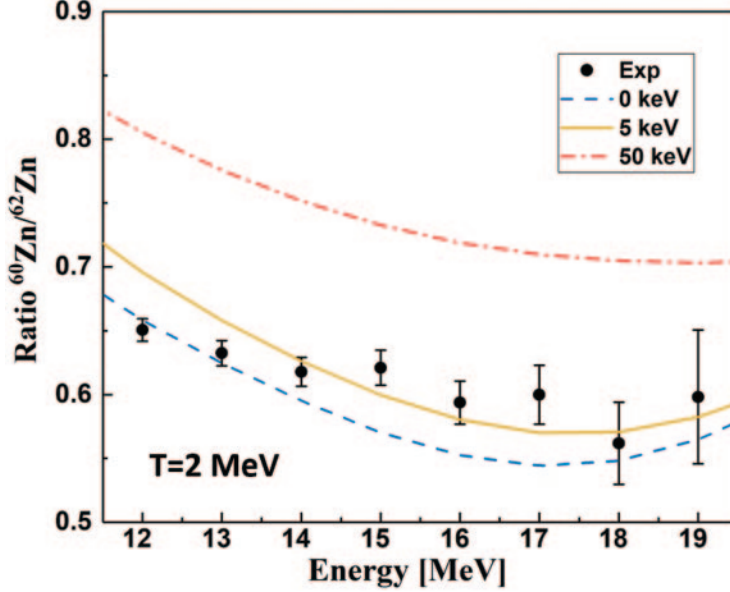


Fig. 2. – Experimental ratio (points) of $^{60}\text{Zn}/^{62}\text{Zn}$ for $T = 2$ MeV, together with the statistical model (CASCADE) ratios corresponding to different Coulomb spreading width values (lines). The blue dashed line and the red dot-dashed line are, respectively, the ratios with $\Gamma^\downarrow = 0$ keV and $\Gamma^\downarrow = 50$ keV (the maximum possible value). The yellow line is, instead, the ratio with $\Gamma^\downarrow = 5$ keV (for $T = 2$ MeV). The result of the minimization of the χ^2 is, indeed, $\Gamma^\downarrow = 5 \pm 3$ keV, for the lower temperature, and $\Gamma^\downarrow = 7 \pm 3$ keV, for the higher temperature.

errors. The experimental ratio, for $T = 2$ MeV, is shown in fig. 2 together with the statistical model (CASCADE) ratios corresponding to different Coulomb spreading width values. The blue dashed line and the red dot-dashed line are, respectively, the ratios with $\Gamma^\downarrow = 0$ keV and $\Gamma^\downarrow = 50$ keV (the maximum possible value). The yellow line is, instead, the ratio with $\Gamma^\downarrow = 5$ keV, the value that best reproduces the experimental trend, following the χ^2 minimization.

The best fit, indeed, gives $\Gamma^\downarrow = 5(3)$ keV at $T = 2$ MeV and $\Gamma^\downarrow = 7(3)$ keV at $T = 2.4$ MeV. The error bars are obtained by the combination of two different uncertainties: one comes from the propagation of the errors in the determination of the GDR parameters and the other by the minimization procedure. The experimental spectrum for ^{60}Zn at $T = 2$ MeV (red points) and the best fit with statistical model (red line) is displayed in the upper part of fig. 1.

In fig. 3, the measured value of Γ^\downarrow is compared with the values available in the literature. For the sake of visibility, we reported the mean value between our two results, that is $\Gamma^\downarrow = 6 \pm 2$ keV. Our datum (orange square) is in good agreement with the experimental trend. At the top right corner, there is a log scale zoom in the region of mass 60. This result confirms firstly that the Coulomb spreading width is a quantity rather independent of temperature [23, 24] and secondly that the Coulomb spreading width extracted from the GDR analysis is very similar in size to the IAS width. This indicates that they come from the same physical mechanism [25, 26].

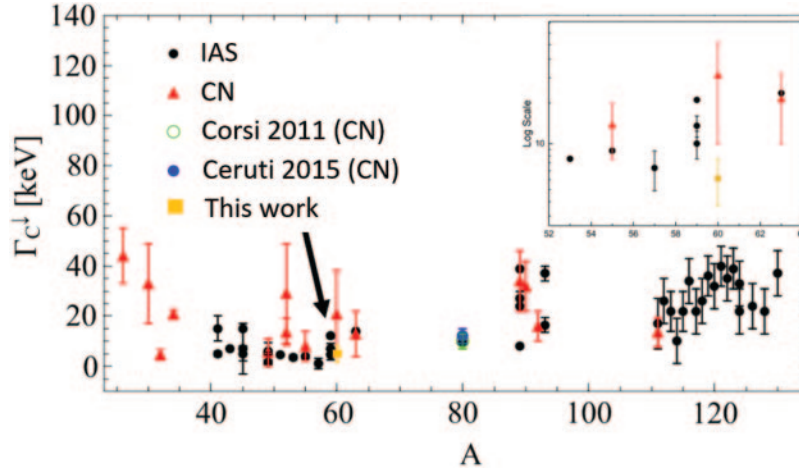


Fig. 3. – Values of the Coulomb spreading width obtained in the IAS (black dots) and in the CN (red triangle) [27, 28]. The blue and green points are the values obtained in [29] and [15], while the orange square is the value obtained in this work. At the top right corner, there is a log scale zoom in the region of the obtained point.

3.3. Mixing probability. – Through the parametrization reported in [28] and implemented in the CASCADE code, we expressed the degree of mixing at angular momentum $J = 0$ and we obtained a value of $\alpha_{>}^2 = (2.1 \pm 1.2)\%$ at $T = 2$ MeV and $\alpha_{>}^2 = (1.8 \pm 0.8)\%$ at $T = 2.4$ MeV. These results support the concept that the mixing probability is a dynamical mechanism in the nucleus, governed by the lifetime of the system and thus it decreases with the excitation energy.

We used the model of ref. [30], which describes the variation of the mixing probability with T , to compare the two data for ^{60}Zn at finite T with the predictions for the ground state. The isospin-mixing probability for a nucleus at finite temperature is defined as

$$(5) \quad \alpha_{>}^2(T) = \frac{1}{I_0 + 1} \frac{\Gamma_{IAS}^{\downarrow}}{\Gamma_{CN}(T) + \Gamma_{IVM}(IAS)},$$

where $\Gamma_{IAS}^{\downarrow}$ is the width of the IAS, to be considered equal to $\Gamma_{>}^{\downarrow}$, $\Gamma_{IVM}(IAS)$ is the width of the Isovector Monopole Resonance (IVM) at the excitation energy of the IAS, which is expected to be constant with T and Γ_{CN} is the compound nucleus decay width that increases with T . We fixed $\Gamma_{IVM}(IAS) = 240$ keV, as reported in [3, 30, 15, 14].

In fig. 4 the value of $\alpha_{>}^2$ calculated using eq. (5) is shown as a function of T . The red band is calculated with a $\Gamma_{>}^{\downarrow} = 6 \pm 2$ keV, corresponding to the average of the two experimental values. Following the discussion in ref. [30], we also considered a weak linear dependence on T of the Coulomb spreading width given by $\Gamma_{>}^{\downarrow}(T) = \Gamma_{>}^{\downarrow}(1 + cT)$. In this expression the chosen slope parameter is $c = 0.1 \text{ MeV}^{-1}$, as reported in [14]. The blue band in fig. 4 displays the dependence of $\alpha_{>}^2$ on T when such weak dependence of $\Gamma_{>}^{\downarrow}$ is considered. The yellow star is the value at $T = 0$ predicted in [31] and the black squares are the values obtained in this analysis with the related error bars. With this calculation, we deduced the mixing probability at $T = 0$, resulting in $\alpha_{>}^2 = 2.5\% \pm 0.8\%$, in good agreement with the prediction in ref. [31].

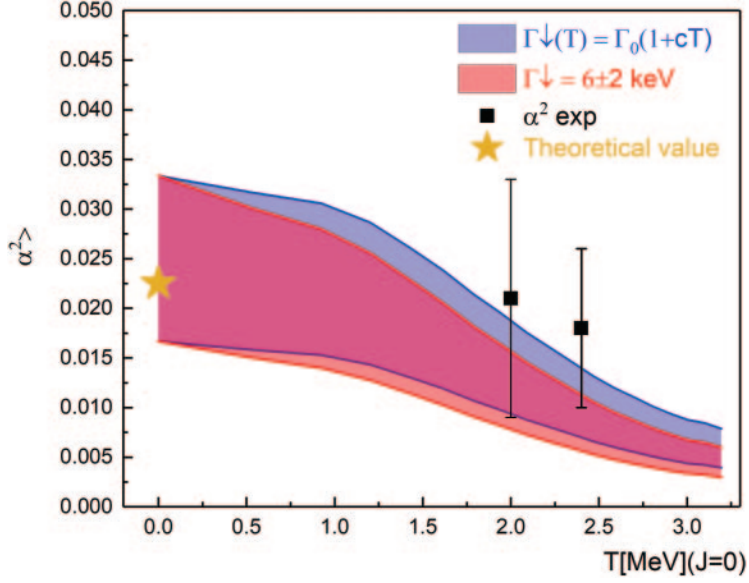


Fig. 4. – Predicted values of $\alpha^2_{>}$ with temperature, for the ^{60}Zn nucleus, together with the experimental points at different temperatures and the prediction at $T = 0$ reported in [31].

For the β -decay, the isospin impurity of states gives an important correction factor to the Fermi transition rates from which the first element of the Cabibbo-Kobayashi-Maskawa (CKM) matrix is deduced. The most precise value of the first term of the CKM matrix, V_{ud} , is obtained from the ft values of $0^+ \rightarrow 0^+$ super-allowed Fermi β -decays with several small corrections. One of these corrections, δ_C , depends on the isospin mixing [1, 2]. In [33] a simple analytic relation between the isospin-mixing-breaking correction term δ_C for the first term (V_{ud}) of the CKM matrix and the isospin-mixing probability is deduced. δ_C is not measurable directly and it is linked to the isospin-mixing coefficient as follows:

$$(6) \quad \delta_C = 4(I + 1) \frac{V_1}{41\xi A^{2/3}} \alpha^2,$$

where $V_1 = 100 \text{ MeV}$ and $\xi = 3$, while α^2 is the isospin impurity in the ground state and I is the isospin of the nucleus. From this equation, we obtained the value $\delta_C = 0.53(17)\%$ for ^{60}Zn . The isospin-mixing correction δ_c , as a function of the nuclear mass number A , is shown in fig. 5. The dashed black line is the prediction from the Damgaard model [34], while the red line is a shell model with Saxon-Woods radial wave function prediction [35]. Black circles are the experimental points extracted from the β -decay, as reported in ref. [1], the blue triangle is the value obtained from the mass measurement in ref. [32]. The red star at mass 80 is the value obtained in [29], whilst the red star at mass 60 is the value of δ_c extracted in this work. The quantity $\frac{\delta_c}{(I+1)}$ is plotted since β -decay measurements are for $I = 1$ nuclei, while that for ^{60}Zn is $I = 0$.

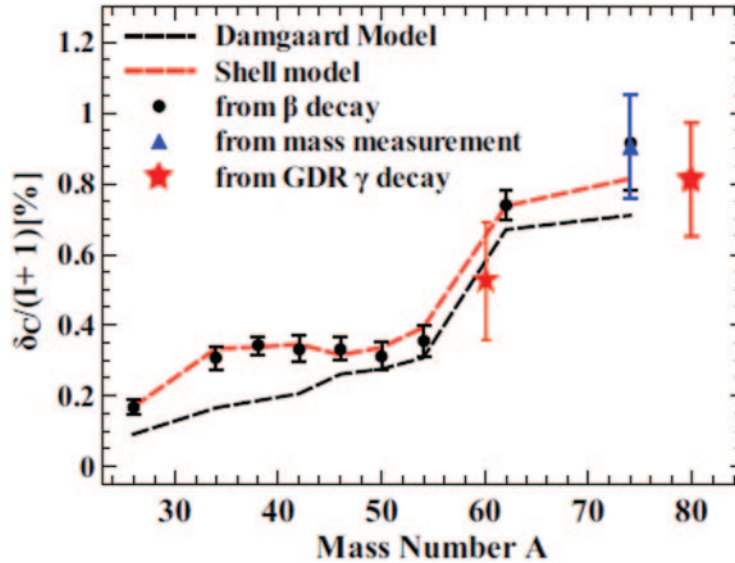


Fig. 5. – The isospin-mixing correction δ_c , as a function of the nuclear mass number A , is shown. The dashed black and red lines are, respectively, the Damgaard model [34] and the shell model [35] predictions. The red star at mass 80 is the value obtained in [29], whilst the red star at mass 60 is the value of δ_c extracted in this work. Black circles and the blue triangle are the experimental points extracted from the β -decay [1] and from the mass measurement [32], respectively.

4. – Conclusion

In conclusion, the temperature dependence of the isospin mixing was obtained for the ^{60}Zn nucleus. The value at temperature $T = 0$ was deduced from the present experiments and it was found to provide a stringent test to theory. Our result also provides the isospin correction term which is used in the β -decay analysis. The latter is found to be in good agreement with the trend of the theoretical values and of mass measurements. The result of this work supports the validity of the method based on the GDR at finite T to obtain isospin mixing. This technique has the merit to allow to access nuclei with $N = Z$ in regions of Z not directly accessible at temperature $T = 0$.

* * *

The author acknowledges tutor Franco Camera and co-tutor Angela Bracco. The author would like to thank the staff of the LNL Legnaro facility and all the participants in the experiment.

REFERENCES

- [1] TOWNER I. S. and HARDY J. C., *Phys. Rev. C*, **82** (2010) 065501.
- [2] SATUŁA W., DOBACZEWSKI J., NAZAREWICZ W. and RAFALSKI M., *Phys. Rev. Lett.*, **106** (2011) 132502.
- [3] SUZUKI T., SAGAWA H. and COLÒ G., *Phys. Rev. C*, **54** (1996) 2954.
- [4] BENTLEY M. A. and LENZI S. M., *Prog. Part. Nucl. Phys.*, **59** (2007) 497.
- [5] WARNER D. D., BENTLEY M. A. and VAN ISACKER P., *Nat. Phys.*, **2** (2006) 311.
- [6] FARNEA E., *Phys. Lett. B*, **551** (2003) 56.

- [7] SEVERIJNS N., *Phys. Rev. C*, **71** (2005) 064310.
- [8] WILKINSON D. H., *Philos. Mag.*, **1** (1956) 379.
- [9] HARAKEH M. N. *et al.*, *Phys. Lett. B*, **176** (1986) 297.
- [10] BRACCO A., *Phys. Rev. Lett.*, **74** (1995) 3748.
- [11] WIELATQUE O., *Phys. Rev. Lett.*, **97** (2006) 012501.
- [12] BRACCO A., LANZA E. G., TAMII A., *Prog. Part. Nucl. Phys.*, **106** (2019) 360.
- [13] BRACCO A., CAMERA F., CRESPI F. C. L., MILLION and WIELATQUE O., *Eur. Phys. J. A*, **55** (2019) 233.
- [14] CERUTI S. *et al.*, *Phys. Rev. C*, **95** (2017) 014312.
- [15] CORSI A. *et al.*, *Phys. Rev. C*, **84** (2011) 041304(R).
- [16] MONDAL D. *et al.*, *Phys. Lett. B*, **763** (2016) 422.
- [17] VALIENTE DOBÒN J., *LNL-INFN annual report 2014* (2015).
- [18] GIAZ A. *et al.*, *Nucl. Instrum. Methods Phys. Res. A*, **729** (2013) 910.
- [19] TESTOV D. *et al.*, *Eur. Phys. J. A*, **55** (2019) 47.
- [20] SKEPPSTEDT O. *et al.*, *Nucl. Instrum. Methods*, **421** (1999) 531.
- [21] PÜHLHOFER F., *Nucl. Phys. A*, **280** (1977) 267.
- [22] BEHR J. A. *et al.*, *Phys. Rev. Lett.*, **70** (1993) 3201.
- [23] HARNEY H. L., RITCHER A. and WEIDENMÜLLER H. A., *Rev. Mod. Phys.*, **58** (1986) 607.
- [24] KUHLMANN E., *Phys. Rev. C*, **20** (1979) 415.
- [25] JÄNECKE J., HARAKEH M. N. and VAN DER WERF S. Y., *Nucl. Phys. A*, **463** (1987) 571.
- [26] COLÒ G., NAGARAJAN M. A., VAN ISACKER P. and VITTURI A., *Phys. Rev. C*, **52** (1995) R1175.
- [27] JÄNECKE J. *et al.*, *Nucl. Phys. A*, **463** (1987) 571.
- [28] HARNEY H. L., RITCHER A. and WEIDENMÜLLER H. A., *Rev. Mod. Phys.*, **58** (1986) 607.
- [29] CERUTI S. *et al.*, *Phys. Rev. Lett.*, **115** (2015) 222502.
- [30] SAGAWA H., BORTIGNON P. F. and COLÒ G., *Phys. Lett. B*, **444** (1998) 1 and private communication.
- [31] SATUŁA W., DOBACZEWSKI J., NAZAREWICZ W. and RAFALSKI M., *Phys. Rev. Lett.*, **103** (2009) 012502.
- [32] KELLERBAUER I. *et al.*, *Phys. Rev. Lett.*, **93** (2004) 072502.
- [33] AUERBACH N., *Phys. Rev. C*, **79** (2009) 035502.
- [34] DAMGAARD J., *Nucl. Phys. A*, **130** (1969) 233.
- [35] TOWNER I. S., HARDY J. C. and HARVEY M., *Nucl. Phys. A*, **284** (1977) 269.